Remote Sensing in Ecology and Conservation
Open Access
ZSL LET'S WORK FOR WILDLIFE

ORIGINAL RESEARCH

Habitat metrics based on multi-temporal Landsat imagery for mapping large mammal habitat

Julian Oeser[1], Marco Heurich[2,3], Cornelius Senf[1], Dirk Pflugmacher[1], Elisa Belotti[4,5] & Tobias Kuemmerle[1,6]

[1]Geography Department, Humboldt-Universität zu Berlin, Berlin, Germany
[2]Bavarian Forest National Park, Grafenau, Germany
[3]Chair of Wildlife Ecology and Management, Faculty of Environment and Natural Resources, University of Freiburg, Freiburg, Germany
[4]Faculty of Forestry and Wood Sciences, Czech University of Life Sciences Prague, Prague, Czechia
[5]Department of Research and Nature Protection, Šumava National Park Administration, Kašperské Hory, Czechia
[6]Integrative Research Institute on Transformation in Human Environment Systems, Humboldt-Universität zu Berlin, Berlin, Germany

Keywords
Habitat, Landsat, large mammal, metrics, spectral-temporal, suitability

Correspondence
Julian Oeser, Geography Department, Humboldt-Universität zu Berlin, Unter den Linden 6, 10099 Berlin, Germany. Tel: +49 (0)30 2093-6806; Fax: +49 (0)30 2093-6848; E-mail: julian.oeser@geo.hu-berlin.de

Editor: Nathalie Pettorelli
Associate Editor: Dolors Armenteras

Received: 1 April 2019; Revised: 28 June 2019; Accepted: 2 July 2019

doi: 10.1002/rse2.122

Remote Sensing in Ecology and Conservation 2020;**6** (1):52–69

Abstract

Up-to-date and fine-scale habitat information is essential for managing and conserving wildlife. Studies assessing wildlife habitat commonly rely on categorical land-cover maps as predictors in habitat models. However, broad land-cover categories often do not adequately capture key habitat features and generating robust land-cover maps is challenging and laborious. Continuous variables derived directly from satellite imagery provide an alternative for capturing land-cover characteristics in habitat models. Improved data availability and processing capacities now allow integrating all available images from medium-resolution sensors in compositing approaches that derive spectral-temporal metrics at the pixel level, summarizing spectral responses over time. In this study, we assessed the usefulness of such metrics derived from Landsat imagery for mapping wildlife habitat. We categorize spectral-temporal metrics into *habitat metrics* characterizing different aspects of wildlife habitat. Comparing the performance of these metrics against categorical land-cover maps in habitat models for lynx, red deer and roe deer, we found that models using habitat metrics consistently outperformed models based on categorical land-cover maps, with average improvements of 13.7% in model AUC and 9.7% in the Continuous Boyce Index. Performance increases were larger for seasonal habitat models, indicating that the habitat metrics capture intra-annual variability in habitat conditions better than land-cover maps. Comparing suitability maps to ancillary data further revealed that our habitat metrics were sensitive to fine-scale heterogeneity in habitat associated with forest structure. Overall, our study highlights the considerable potential of Landsat-based spectral temporal metrics for assessing wildlife habitat. Given these metrics can be derived directly and in an automatized fashion from globally and freely available Landsat imagery, they open up new possibilities for monitoring habitat dynamics in space and time.

Introduction

Habitat maps can provide critical information for wildlife management and conservation planning (Margules and Pressey 2000; Sutherland et al. 2004). Such maps are typically derived using correlative habitat models (i.e. species distribution models, environmental niche models or resource selection functions) (Boyce and McDonald 1999; Guisan and Zimmermann 2000; Elith et al. 2006). Habitat models can improve the understanding of a species' ecology while providing data on their actual or potential distribution (Guisan and Thuiller 2005; Elith and Leathwick 2009), which, in turn, are important indicators for assessing biodiversity change (Pereira et al. 2013; Jetz et al. 2019). Moreover, habitat suitability maps often are the basis for downstream-analyses, such as modeling

population dynamics or assessing landscape fragmentation and connectivity (Larson et al. 2004; Zeller et al. 2012). Thus, habitat models are particularly valuable if they can be applied across large areas (McDermid et al. 2005) and with regular repeat intervals (Pressey et al. 2007).

Most studies mapping wildlife habitat use categorical land-cover maps derived from satellite imagery as spatial predictor variables (Pearson et al. 2004; Thuiller et al. 2004; Zuckerberg et al. 2016). The frequent use of land-cover maps can likely be attributed to the wide availability of freely available map products (Wulder et al. 2018), as well as their easy interpretability. However, using land-cover maps for habitat assessments also comes with several limitations. First, available broad-scale land-cover maps have predefined, typically coarse thematic legends that do not necessarily reflect a species' habitat requirements (Bradley and Fleishman 2008; Coops and Wulder 2019). Otherwise, land-cover maps can be created for a specific purpose, but doing so is laborious, requires considerable technical expertise and adequate reference datasets. Second, a classification of the spectral information contained in satellite images implies a loss of information (Krishnaswamy et al. 2009). Thus, fine-scale gradients of habitat suitability associated with variation within land-cover classes (e.g. forest composition and structure) might be missed by categorical maps. Finally, satellite-based land-cover maps always contain errors (Powell et al. 2004; Pflugmacher et al. 2011), which are typically not accounted for in habitat models (Cord et al. 2014).

Alternatively, continuous variables derived directly from satellite images, such as vegetation indices (Pettorelli et al. 2005, 2011), can be used as predictors in habitat models (Coops and Wulder 2019; Leitão and Santos 2019). Several studies have demonstrated the usefulness of Landsat imagery in this context (Lahoz-Monfort et al. 2010; Shirley et al. 2013; West et al. 2017). In contrast to coarser resolution sensors, Landsat imagery allows resolving fine-scale habitat features (Shirley et al. 2013; Remelgado et al. 2018). Moreover, the Landsat archive provides freely available, global imagery back to the 1970s (Wulder et al. 2016, 2019), which should represent major opportunities for assessing wildlife habitat in space and time (Nagendra et al. 2013; He et al. 2015). However, using Landsat imagery also comes with distinct challenges, which likely explains its relatively limited use in habitat assessments so far. On one hand, the comparably low temporal resolution of Landsat (16-day revisit time for a single satellite) can make the selection of suitable individual images difficult or even impossible due to cloud cover. On the other hand, the combination of many Landsat images in space or time can imply considerable technical challenges and computational costs (Young et al. 2017). While time series-based approaches have been widely adopted for characterizing habitat with coarse resolution sensors such as MODIS (Coops et al. 2009; Cord and Rödder 2011; Bischof et al. 2012), Landsat-based habitat studies instead have frequently relied on images-based analysis of only a single or few selected images (Lahoz-Monfort et al. 2010; but see Jantz et al. 2016; Remelgado et al. 2018).

Recently, the provision of Landsat data in analysis-ready formats (Dwyer et al. 2018; Wulder et al. 2019) and rapidly improving computational capacities (e.g. through cloud computing platforms; Gorelick et al. 2017), have dramatically improved the possibilities for analyzing large sets of Landsat images. One development underpining these advances is the shift from image-based analyses to the increasing use of pixel-based compositing approaches (Potapov et al. 2011; Hansen et al. 2014; Bleyhl et al. 2017). In one such compositing approach, all available images in a time frame are combined by calculating pixel-wise, spectral-temporal metrics to create cloud-free composite images summarizing spectral responses over time (Griffiths et al. 2013; Gómez et al. 2016; Pflugmacher et al. 2019). While Landsat metric-based composites have allowed for substantial progress in land-cover mapping (Azzari and Lobell 2017), their usefulness for assessing wildlife habitat via habitat models remains largely unexplored.

In this study, we investigate the potential of Landsat-based spectral-temporal metrics for mapping large mammal habitat and compare them against land-cover maps. Large mammals play crucial roles in structuring ecosystems (Ripple et al. 2014, 2015), and often are important focal species for conservation (Sergio et al. 2006; Clucas et al. 2008; Branton and Richardson 2011). However, their conservation is particularly challenging, as they require extensive habitats (Cardillo et al. 2005) and often come into conflict with humans (Treves and Karanth 2003; Young et al. 2005). Thus, pro-active management and monitoring of their populations is important, which requires timely and detailed spatial information on habitat across large areas.

We mapped habitat suitability for a large carnivore (Eurasian lynx; *Lynx lynx*) and two large herbivores (red deer, *Cervus elaphus;* and roe deer, *Capreolus capreolus*) in the Bohemian Forest Ecosystem in Germany and Czechia, using spectral-temporal metrics derived from Landsat imagery together with large GPS tracking datasets in habitat models. To improve the usefulness of spectral-temporal metrics for habitat mapping, we categorize spectral-temporal metrics into groups of *habitat metrics* specifically targeting key aspects of large mammal habitat. We test these habitat metrics as predictors in habitat models and compare their performance against models based on categorical land-cover maps. Specifically, we ask the following research questions:

1 Do habitat metrics improve the predictive performance of habitat models compared to land-cover maps?
2 Can habitat suitability maps based on habitat metrics capture fine-scale variation in habitat related to forest structure?
3 Do habitat models based on habitat metrics capture differences in habitat use between lynx, red deer and roe deer and across seasons?

Material and Methods

Study area

The Bohemian Forest Ecosystem is a low-elevation, forested mountain chain approximately 130 km long and 60 km wide, situated along the border of Austria, Czechia and Germany (Fig. 1). Two protected areas form the center of the study area: The Bavarian Forest National Park (240 km²) and the Šumava National Park (690 km²). These protected areas are mostly forested, while their surroundings consist of mosaics of smaller forest patches, meadows, cropland and villages. Roe deer and red deer are widely distributed in the area (Heurich et al. 2015) and Eurasian lynx has been reintroduced in the 1970s (Wölfl et al. 2001). Lynx mainly prey on roe deer and to a much lesser extent on red deer (Belotti et al. 2015).

Wildlife data

As information on species presence, we used a large GPS tracking dataset from radio-collared lynx (seven individuals), red deer (41 individuals) and roe deer (82 individuals), collected between 2011 and 2013. To account for seasonal changes in habitat selection (Godvik et al. 2009; Dupke et al. 2016; Filla et al. 2017), we fitted separate models using presence data from the entire year (hereafter: year-round models) as well as seasonal models using presence data only from winter or summer (Table 1; hereafter: summer and winter models). Summer observations included all GPS recordings collected between 1 April and 31 October, winter observations all recordings between 1 November and 31 March (Godvik et al. 2009; Filla et al. 2017). Since some of the radio-collared red deer are kept in enclosures during winter (Rivrud et al. 2016), we removed red deer locations inside winter enclosures. To reduce spatial auto-correlation, we randomly selected one location per day and individual for each dataset (Magg et al. 2015; Holloway and Miller 2017). The size of our final presence datasets used for building habitat models ranged from ca. 1000 locations for the lynx winter model to ca. 18 000 locations for the roe deer year-round model (Table 1).

Landsat-based habitat metrics

To characterize large mammal habitat directly from multi-temporal Landsat imagery, we derived a set of spectral-temporal metrics (Hansen et al. 2014; Azzari and Lobell 2017; Pflugmacher et al. 2019) describing different aspects of wildlife habitat. These composite images are generated from time series of spectral indices by calculating pixel-level statistical indicators summarizing the spectral

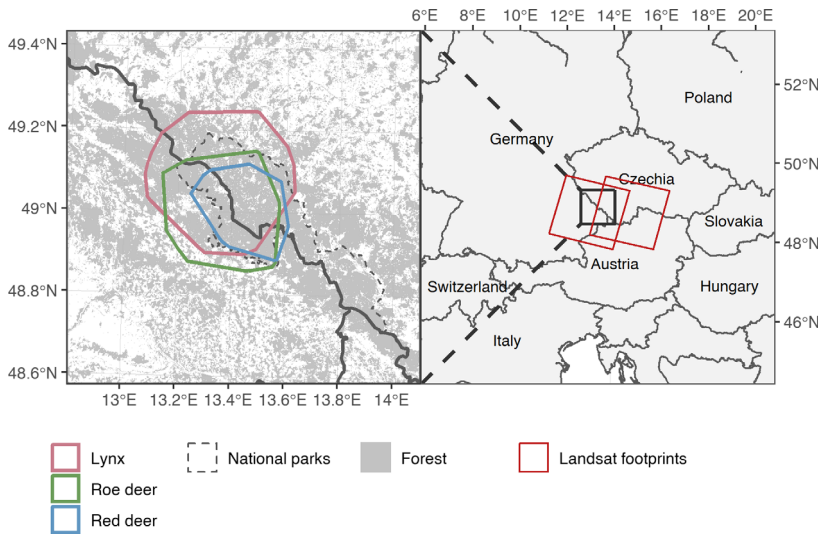

Figure 1. Map of the study area (left) including Minimum Convex Polygons derived from all lynx, red deer and roe deer locations (see Wildlife data), with forested areas highlighted in grey. Overview map (right) showing the location of the study region, national parks and the used Landsat footprints.

Table 1. Summary of the wildlife data (GPS telemetry observations) used as presence information in our habitat models.

Species	No. of individuals	No. of year-round observations	No. of summer observations	No. of winter observations
Lynx	7	2671	1629	1042
Red deer	41	10 329	7648	2681
Roe deer	82	18 151	10 215	7936

properties of all imagery in a given time window (Fig. 2). Based on available studies linking satellite-derived variables to wildlife habitat characteristics (Table 2), we then categorize these spectral-temporal metrics into groups of *habitat metrics* relating to different aspects of wildlife habitat. For calculating metrics, we used all available Collection 1 Tier 1 surface reflectance images from the Landsat sensors 5 TM, 7 ETM+ and 8 OLI recorded between 2011 and 2013 (165 images across two Landsat footprints). The Tier 1 surface reflectance product contains atmospherically corrected data (Masek et al. 2006; Vermote et al. 2016) with the lowest georegistration errors (Young et al. 2017). To account for different Landsat sensor specifications, we used the coefficients provided by Roy et al. (2016) to cross-calibrate Landsat 8 surface reflectance data to Landsat 7 reflectance values. We performed all processing of Landsat imagery, including metric calculation, in the Google Earth Engine (Gorelick et al. 2017; see Supporting Information for Google Earth Engine code).

For every Landsat image, we calculated (1) the Tasseled Cap (TC) components greenness, brightness and wetness (Crist and Cicone 1984), and (2) binary snow masks created from quality flags in the Pixel-Quality Assessment (QA) band derived from the CFMask algorithm (Foga et al. 2017). For calculating the TC components, we masked out all observations containing clouds, cloud shadows or snow using the respective flags in the QA-band and used the coefficients for surface reflectance data provided in Crist (1985). The TC components capture different spectral characteristics describing land-cover features (Crist and Cicone 1984; Pasquarella et al. 2016). For example, greenness relates to the amount of photosynthetically active vegetation, similar to vegetation indices such as NDVI (De Jong 1994). Brightness has been linked to albedo (e.g. open habitats including bare soil, certain agricultural crops and built-up areas; Yang and Liu 2005). Wetness has been associated with vegetation and soil moisture (Crist and Cicone 1984), but is also widely used to capture forest characteristics and disturbances (Cohen et al. 1995; Hansen et al. 2001; Jin and Sader 2005).

We summarized Tasseled Cap greenness, brightness and wetness over time by calculating a set of robust statistical metrics (median, interquartile and interdecile range, and Theil-Sen slope; see Table 2; Flood 2013). To capture spectral variations throughout the year, we calculated metrics using all available images, on the one hand, and images from specific temporal windows within the year, on the other. We set the temporal windows to represent key phenological stages in our study region (Senf et al. 2017), which should help capturing important habitat characteristics, such as vegetation types or food availability (Hamel et al. 2009; Remelgado et al. 2018). For defining the temporal windows, we used the day of year (DOY) of image recording to categorize Landsat images into start-of-season (DOY 60-151, 42 images), peak-of-season (DOY 152-243, 53 images), and end-of-season observations (DOY 244-334, 54 images). We also tested metrics based on DOY 335 - 59 observations, but omitted them from further analysis due to persistent cloud and snow cover leading to low observation numbers during winter in our study area. To describe the rate of vegetation green-up, we used the Theil-Sen approach (Theil 1992; Fernandes and Leblanc 2005) for estimating the rate of change in greenness values during spring. Previous studies have linked vegetation productivity increase during spring to forage quality for large herbivores (Pettorelli et al. 2007; Hamel et al. 2009). As a measure of snow-cover frequency, we divided the number of observations flagged as snow by the number of clear observations for each pixel. A comparison of the Landsat-derived snow-cover frequency against the MODIS snow-cover product (Hall et al. 2010) showed overall good agreement between both datasets (see Supporting Information).

In total, our set of metrics included 14 variables (Table 2), which we categorized into five groups of habitat metrics: (1) productivity (based on TC greenness), (2) phenology (based on variability in greenness), (3) openness (based on TC brightness), (4) moisture (based on TC wetness), and (5) snow cover.

Land cover mapping

To compare the usefulness of our habitat metrics for assessing large mammal habitat against categorical land-cover maps, we derived two land-cover maps for our study region. First, we mapped land cover for the target year 2012 by applying a random forest classifier (Breiman 2001) to the set of habitat metrics. This map thus represents a site-specific land-cover map, which are sometimes produced for habitat assessments (Kuemmerle et al. 2010; Bleyhl et al. 2017). We sampled training pixels within reference polygons that were digitized based on (1) aerial surveys (Gonzalez et al. 2018) and (2) high-resolution imagery in Google Earth. We mapped 13 land-cover classes: broadleaf forest,

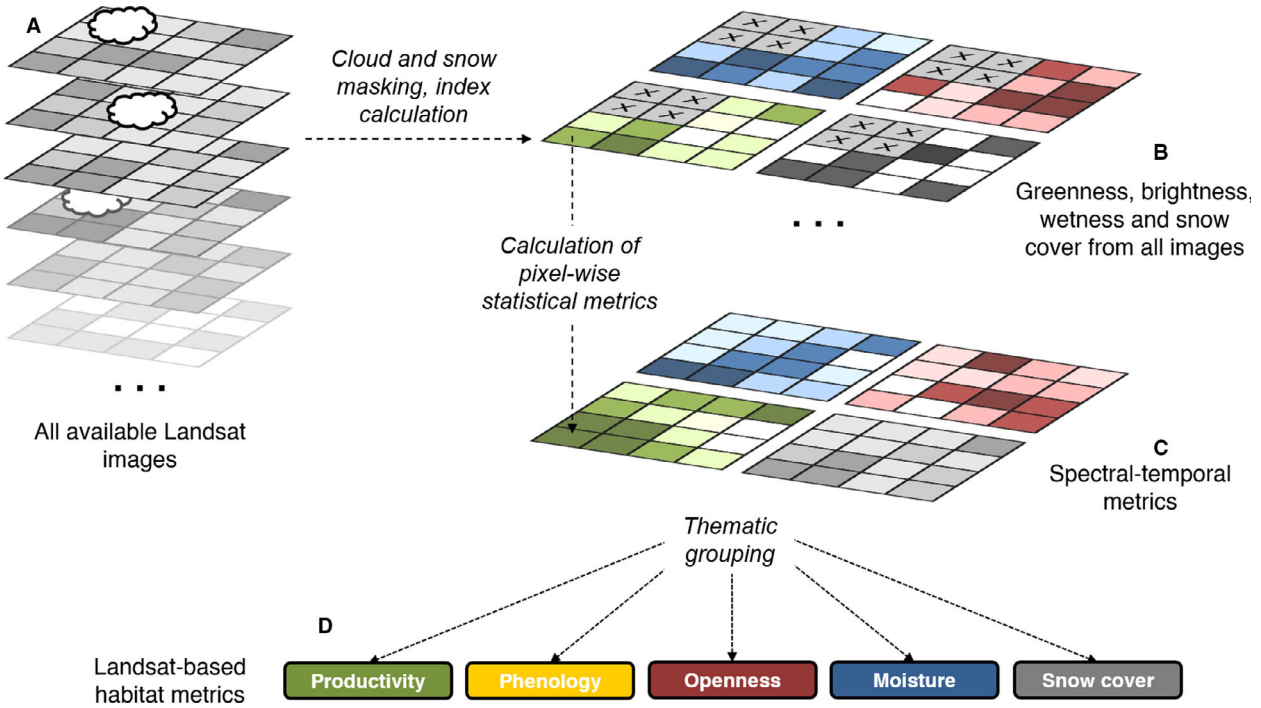

Figure 2. Illustration of habitat metrics calculation. (A) All available, pre-processed (e.g. atmospherically corrected) images are acquired. (B) Invalid observations (e.g. clouds, snow) are masked and spectral indices (in our case Tasseled Cap greenness, brightness and wetness, as well as snow masks) are derived. (C) These indices are summarized at the pixel level using different statistical metrics (e.g. median, interquartile range). (D) The resulting spectral-temporal metrics are then categorized into habitat metrics characterizing different aspects of wildlife habitat (productivity, phenology, openness, moisture and snow cover).

built-up, clear-cut, coniferous forest, cropland, deadwood, forest regrowth, grassland, mixed forest, natural grassland, rock, shrub and water. The resulting land-cover map was validated using a set of independent test pixels not used for training and had an overall accuracy of 91.5% (see Supporting Information for a more detailed description of the classification and validation procedure).

As a second land-cover map, we downloaded the CORINE land-cover dataset (Büttner et al. 2004) for the year 2012, representing a broad-scale, general land-cover product. This European-wide land-cover map is available at a spatial resolution of 100 m and is frequently used to map habitat suitability for large mammals in Europe (Schadt et al. 2002; Magg et al. 2015; Kuemmerle et al. 2018). The CORINE data for our study area included a total of 27 classes on five major land-cover types (artificial surfaces, agricultural areas, forest and semi-natural areas, wetlands and water bodies; see Table S2).

Parametrization of habitat models

We fitted habitat models for lynx, red deer and roe deer using maximum entropy (Maxent) modeling (Phillips et al. 2006). Maxent contrasts the values of environmental predictors at presence observations with their overall distribution obtained from a sample of background points (or pseudo-absences; Merow et al. 2013). To generate background points, we randomly sampled 30 000 points inside the Minimum Convex Polygons of presence datasets (Phillips and Dudík 2008; Northrup et al. 2013). We used the R-package *dismo* (Hijmans et al. 2017) for building Maxent models, using all feature classes and a regularization multiplier of $\beta = 1$ (Merow et al. 2013).

For each species, we fitted year-round, summer, and winter habitat models using (1) the set of habitat metrics, (2) site-specific land-cover map created from Landsat imagery, and (3) the CORINE land-cover map. This resulted in a total of nine habitat models per species. To evaluate the predictive performance of our models, we used ten-fold cross-validation. We calculated two performance measures capturing two different aspects of predictive performance: The area under the Receiver Operator Characteristic curve (AUC) as an indicator of discrimination capacity (i.e. how well a model separates presence from background points; Jiménez-Valverde et al. 2013), and the Continuous Boyce Index (CBI; Hirzel et al. 2006) as an indicator of model calibration (i.e. how well predicted suitability values correspond with observed

Table 2. Overview of habitat metrics derived from Landsat imagery.

Habitat metric group	Specific metrics (number of metrics)	Related habitat features
Productivity	Median TC greenness for start-of-season, peak-of-season and end-of-season (3)	Food availability (Pettorelli et al. 2005; Coops et al. 2008)
Phenology	Interquartile and interdecile range of TC greenness based on all observations; Theil-Sen estimator for regression of TC greenness against day of year for start-of-season (3)	Food availability, forage quality (Pettorelli et al. 2007; Hamel et al. 2009)
Openness	Median TC brightness for start-of-season, peak-of-season and end-of-season (3)	Absence of protective cover, food availability (Carroll et al. 2001; Holbrook et al. 2017)
Moisture	Median TC wetness for start-of-season, peak-of-season and end-of-season (3)	Forest type and structure, protective cover, vegetation and soil moisture (Cohen et al. 1995; Roy and Ravan 1996; Hansen et al. 2001)
Snow cover	Frequency of snow cover (relative to number of clear observations) based on all observations, frequency of snow cover during start-of-season (2)	Resource accessibility, movement, predation risk (Michaud et al. 2014; Macander et al. 2015)
Total	14 metrics	

proportions of occupied sites; Phillips and Elith 2010). For assessing changes in predictive performance associated with using the habitat metrics instead of the land-cover maps, we calculated the percent changes in AUC and CBI compared to the best-performing land-cover map for each model. Finally, we derived habitat suitability maps from each Maxent model by creating spatial predictions, using the bounding box of all GPS telemetry locations as a reference extent.

Assessing habitat metrics

To assess whether the habitat metrics allow capturing fine-scale habitat characteristics associated with forest structure, we compared (1) the metric values, and (2) the derived suitability maps from year-round models against information on fine-scale forest attributes (i.e. stand age, lying and standing deadwood, type of forest regrowth). For this comparison, we used a high-resolution vegetation type map available for the Bavarian Forest National Park that was created by manual interpretation of aerial imagery (Gonzalez et al. 2018).

To assess whether the habitat metrics allowed capturing differences in habitat use between species and across seasons, we compared the contribution of the different habitat metrics across models. Since the groups of metrics (productivity, phenology, openness, moisture, snow-cover) were selected to characterize different aspects of habitat, their importance in habitat models can be expected to be consistent with known patterns of habitat selection for lynx, red deer and roe deer. We computed permutation importance scores indicating relative variable importance (Searcy and Shaffer 2016). Then, we summed the importance scores of all variables belonging to a metric group and used this group-wise sum as an indicator for the contribution of the habitat metrics to a model. Lastly, we compared the importance of metrics based on the temporal windows used for their computation (i.e. all observations, start of season, peak of season, end of season), by calculating the mean importance of metrics from each temporal window across all habitat models.

Results

Comparison of predictive performance and habitat suitability maps

Models based on our habitat metrics showed higher AUC and CBI values (mean AUC = 0.76, standard error ±0.02; mean CBI = 0.97 ± 0.01) than models based on categorical land-cover maps (mean AUC = 0.60 ±0.03, mean CBI = 0.84 ± 0.03 Fig. 3A). Comparing habitat models based on the two land-cover maps, models using the site-specific map had higher AUC values than CORINE-based models (mean AUC = 0.66 ± 0.02 vs. 0.54 ± 0.06), but slightly lower CBI values (mean CBI 0.82 ± 0.05 vs. 0.85 ± 0.03). Using the habitat metrics improved the predictive performance, both in terms of discrimination capacity (AUC) and model calibration (CBI), of all habitat models relative to the best-performing land-cover based model (Fig. 3C–D). Relative improvements in ranged from 9-23% for AUC values (mean = 13.7), and 3-21% for CBI values (mean = 9.2), showing variations across species and time periods covered. On average, performance increases were larger for seasonal habitat models

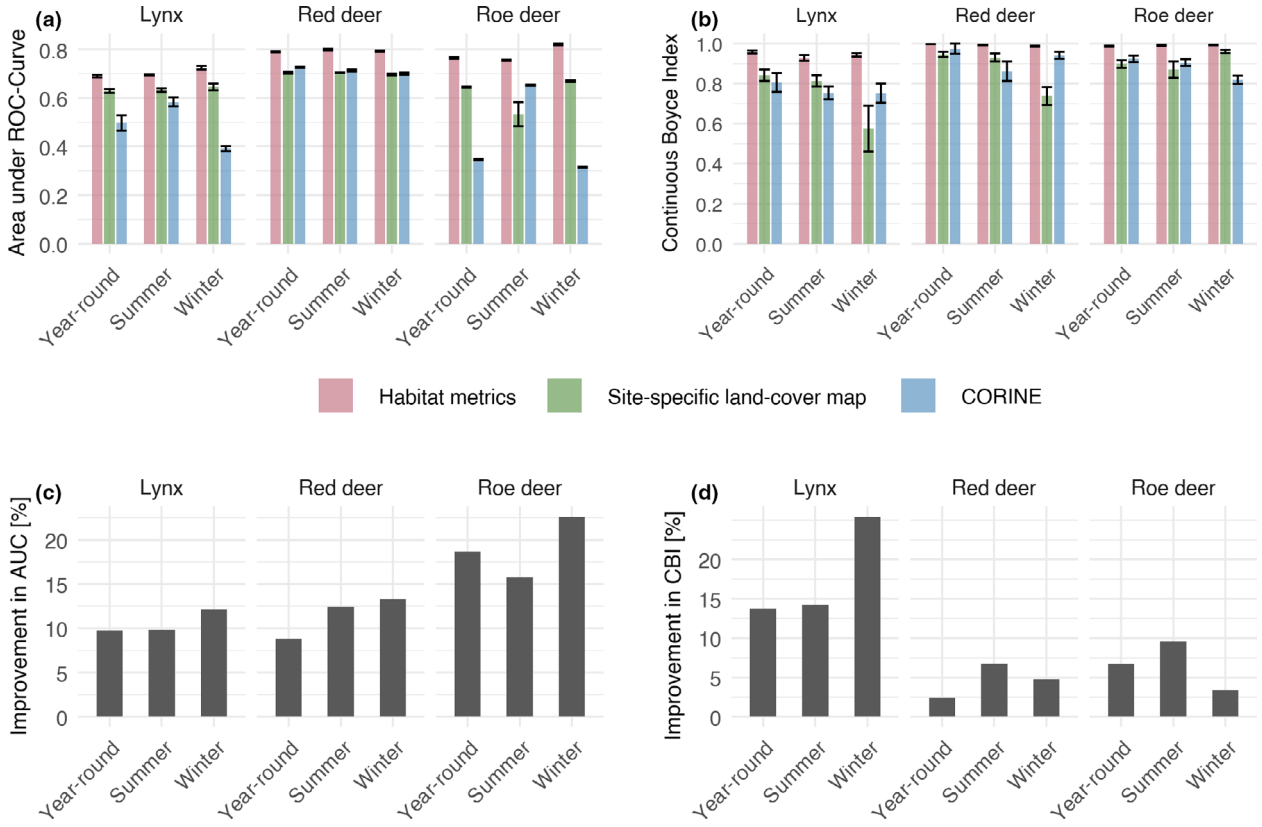

Figure 3. Performance of habitat models based on habitat metrics vs. models based on land-cover maps. (a) Mean AUC across ten cross-validation runs, (b) Mean CBI across ten cross-validation runs, (c) average percent improvement in AUC when comparing the habitat metrics model versus the best-performing land-cover map model, (d) average percent improvement in CBI. Error bars in (A and B) indicate standard errors of the mean.

compared to year-round models (relative improvement in AUC: 14.5% vs. 12.3%; improvement in CBI: 11.3% vs. 5.1%). Performance improvements were also larger for winter models than for summer models (improvement in AUC 16.0% vs. 13.0%; improvement in CBI 12.1% vs. 10.4%). Average improvements in AUC were largest for roe deer (19.0%), improvements in CBI largest for red deer (11.7%).

Overall, spatial patterns of habitat suitability were similar between maps derived from models using the habitat metrics and those based on the land-cover maps (Fig. 4; see Fig. S5–S6). However, some differences were discernible, such as the lower spatial resolution of the CORINE map, as well as variation in habitat suitability within land-cover classes in the map based on the habitat metrics. In addition, suitability maps based on the habitat metrics exhibited striping artifacts corresponding to scan line errors of Landsat 7. These artifacts were most pronounced in areas with persistent cloud cover (i.e. high elevations). We found these striping artifacts mainly to occur in metrics calculated from start-of-season observations (see Fig. S7 for an example).

Variation of habitat suitability with forest structure

The values of habitat metrics varied considerably for classes of forest type and age, and showed patterns consistent with forest type and age characteristics (Fig. 5; see Fig. S8 for comparison with deadwood and forest regrowth classes). For example, openness metrics tended to decrease with stand age. Productivity and phenology metrics tended to be higher for broadleaf forest than for coniferous forest, with differences increasing with stand age, while mixed forests showed intermediate productivity and phenology values.

Next to the metric values themselves, the predicted suitability values also varied with forest structure classes (Fig. 6). For example, lying deadwood had lower suitability for roe deer and lynx than standing deadwood, but a higher

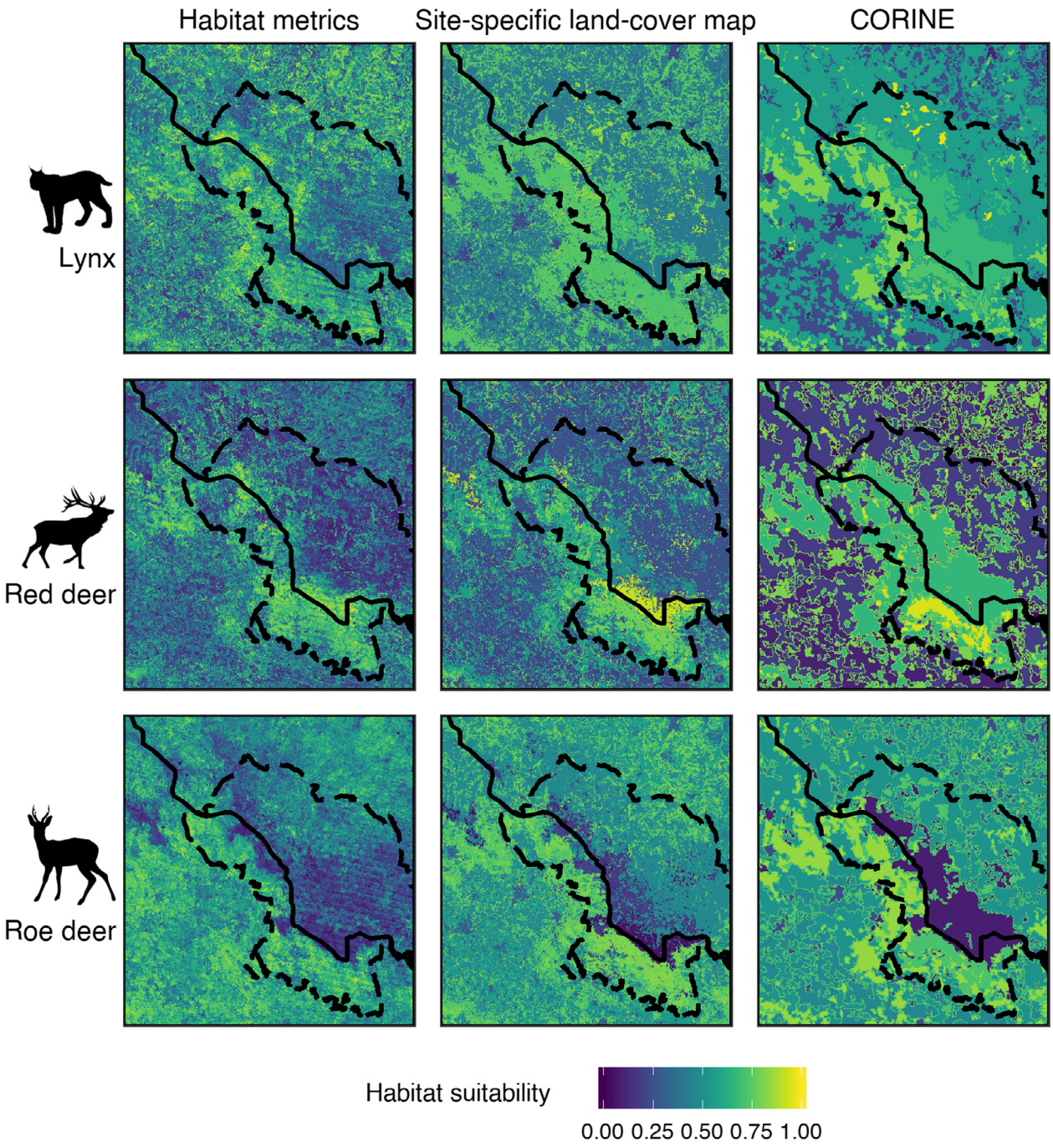

Figure 4. Habitat suitability maps based on year-round habitat models using the habitat metrics (left column), the site-specific land-cover map (middle column) and the CORINE land-cover map (right column) for lynx, roe deer and red deer. Continuous line indicates country border, dashed lines show the extents of the national parks.

suitability for red deer. Habitat suitability for lynx and roe deer varied with the type of regrowth, with higher suitability for broadleaf than for coniferous or mixed regrowth. Finally, habitat suitability for red and roe deer showed relationships with forest age. While suitability generally declined with stand age for red deer, it increased for roe deer.

Importance of different habitat metrics across models

The importance of the different habitat metrics varied markedly between species, and also between models fitted for different time periods (Fig. 7A). For instance, in our

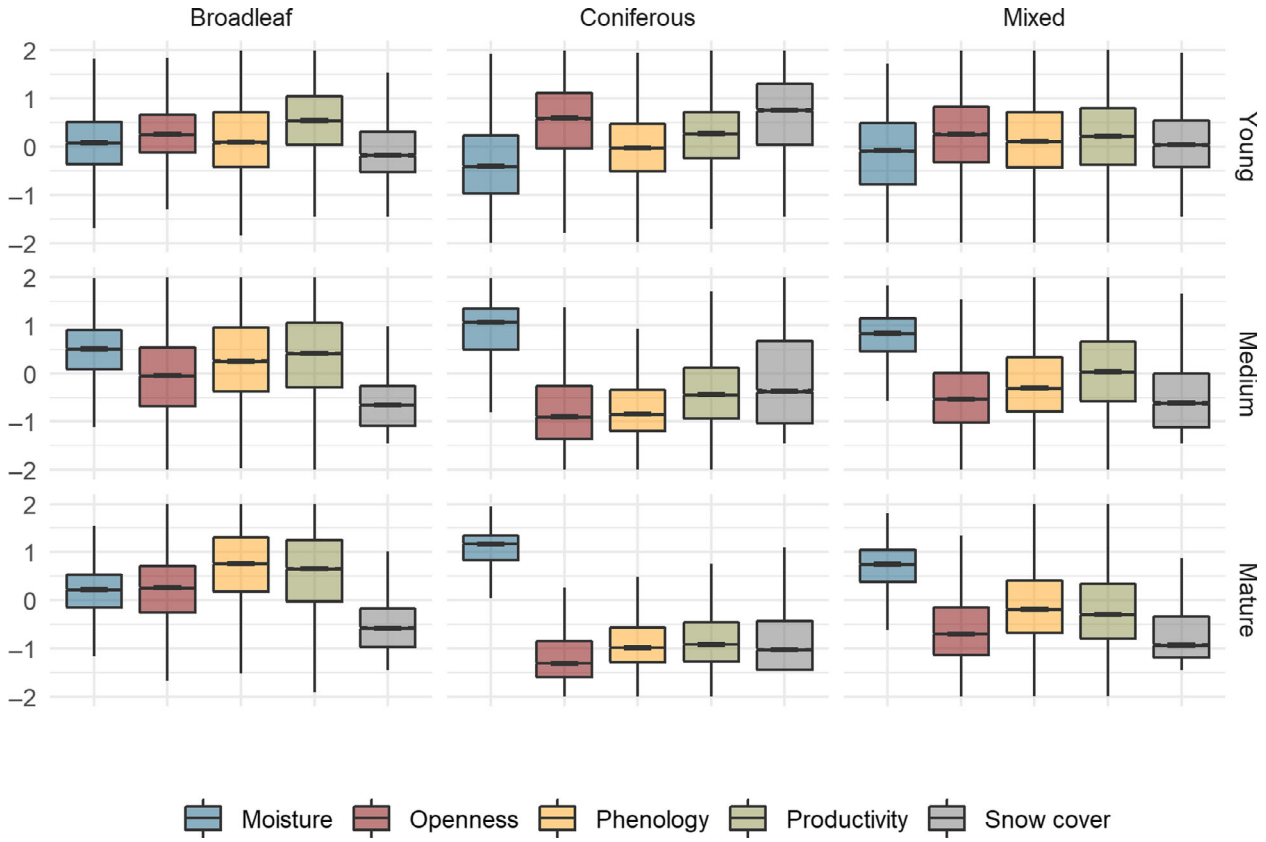

Figure 5. Variation of habitat metric values with forest type and age. All individual metrics were standardized via a *z*-transformation to ensure comparability between spectral indices.

lynx models, the openness metrics were consistently among the most important, while being generally less important in the red and roe deer models. In contrast, the contribution of phenology metrics, relating to forage availability and quality, was much larger in red deer and roe deer models than in lynx models. The contributions of habitat metrics in seasonal models for the three species were consistent with differences in habitat use between summer and winter. For example, snow-cover metrics were more important in winter models than in summer models for all species. Similarly, the phenology metrics were less important in winter models than in summer models for the two deer species. Comparing the importance of metrics calculated from the different temporal windows of Landsat observations, metrics calculated from start-of-season observations were most important in habitat models for all three species, showing particularly high importance scores in models for red and roe deer (Fig. 7B).

Discussion

Our assessment of Landsat-based spectral-temporal metrics in habitat models for lynx, red deer and roe deer yielded four major insights. First, models using the habitat metrics consistently outperformed models based on land-cover maps. Both performance measures (AUC and CBI), indicating discrimination capacity and model calibration, showed considerable increases when compared to models using land-cover maps. This is in line with previous research highlighting the advantages of continuous satellite-derived variables over categorical maps for characterizing species' habitat (Cord et al. 2014; Coops and Wulder 2019). Calculating spectral-temporal metrics from time series of medium-resolution satellite imagery provides for an effective way to generate continuous variables that allow assessing habitat with high levels of spatial detail. Remelgado et al. (2018) previously used seasonal Landsat surface reflectance composites for modeling resource availability for white storks (*Ciconia ciconia*). Our study showcases how spectral-temporal metrics from multiple spectral indices can be linked to different habitat aspects, allowing for a comprehensive and meaningful characterization of wildlife habitat from medium resolution imagery.

Second, the habitat metrics allowed capturing variation in habitat between seasons, which categorical land-cover

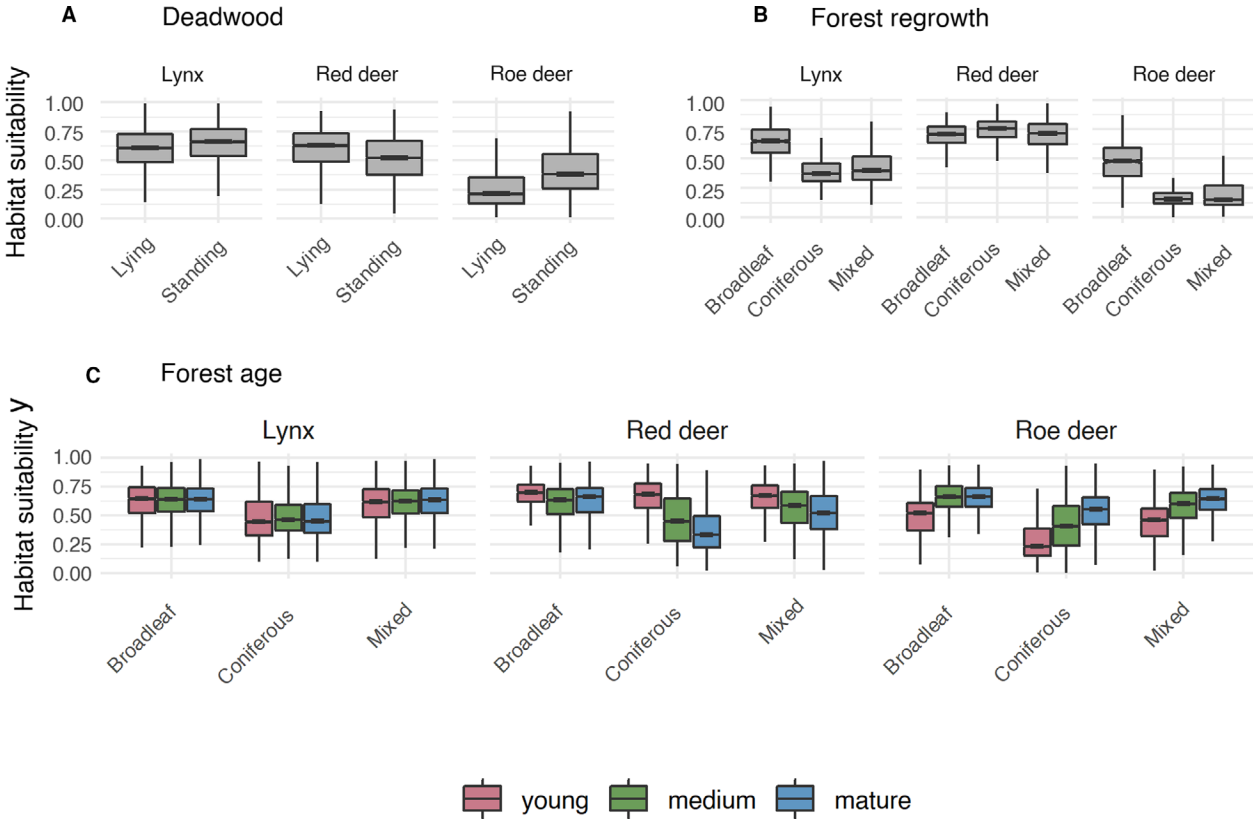

Figure 6. Variation in habitat suitability in models based on habitat metrics for classes capturing forest structure: (A) Different types of deadwood, (B) different types of forest regeneration, and (C) different forest age classes.

maps typically do not reflect. Performance improvements from using habitat metrics instead of land-cover maps were larger for our seasonal models than for year-round models (Fig. 3B). At the same time, metrics relating to intra-annual variability of habitat conditions (e.g. snow cover, phenology) were highly important in our habitat models (Fig. 7A). These results demonstrate that spectral-temporal metrics can be useful to move away from static depictions of habitat. This is important, as many animals adapt their habitat use in reaction to changing habitat conditions throughout the year (Godvik et al. 2009; Dupke et al. 2016; Filla et al. 2017). Accounting for such variation in habitat models can provide useful information for wildlife management and conservation (Brambilla and Saporetti 2014; Frans et al. 2017). Combining high-resolution wildlife tracking data (Kays et al. 2015; Pimm et al. 2015) with satellite time series holds great potential in this regard, since it allows simultaneously describing how habitat conditions vary within a year, and how animals respond to these changes (Bischof et al. 2012; Gschweng et al. 2012).

Third, habitat metrics allowed describing fine-scale heterogeneity in habitat associated with forest structure. The suitability maps based on the habitat metrics were consistent with prior studies on habitat selection of our study species. For instance, roe deer in our study area have been shown to preferentially select older forest stands (Dupke et al. 2016). Likewise, the higher suitability of broadleaf regrowth compared to coniferous regrowth likely is related to the observation that roe deer, as selective browsers, prefer young broadleaved trees for browsing (Kullberg and Bergström 2001; Götmark et al. 2005; Heinze et al. 2011). Conversely, for red deer, being a mixed feeder (Krojerová-Prokešová et al. 2010), the type of regrowth is less influential. Together, this suggests that our habitat metrics were able to characterize fine-scale habitat variation that is extremely difficult to classify in satellite-based land-cover maps (e.g. forest age classes, different types of forest regrowth).

Finally, models using the habitat metrics were able to represent differences in habitat selection between species and seasons, as indicated by the differences in relative variable importance scores among our models. For example, the importance of the openness metrics in our lynx models, with habitat suitability decreasing with increasing brightness, likely reflects the known avoidance of open

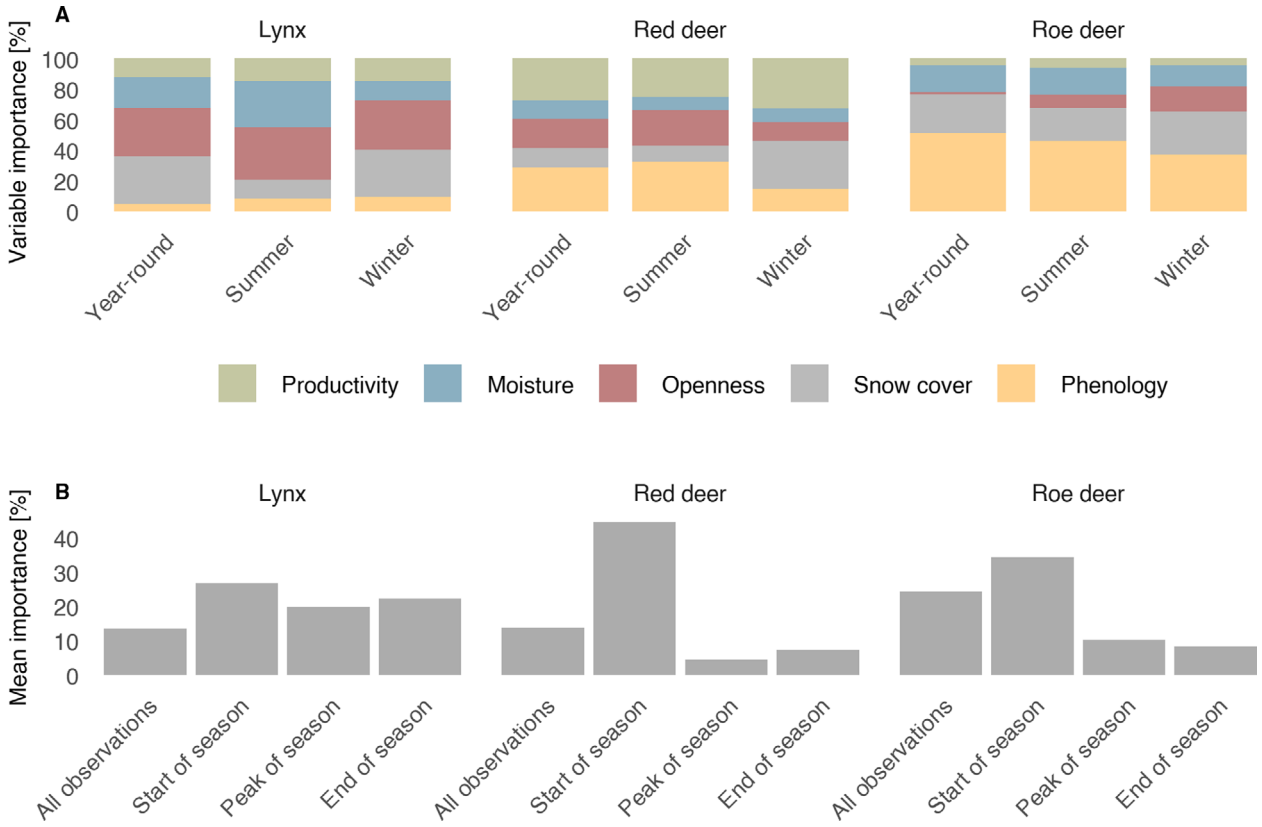

Figure 7. Importance of habitat metrics in lynx, red deer and roe deer habitat models. (A) Sums of permutation importance scores for habitat metrics in year-round, winter and summer habitat models. (B) Mean variable importance score of metrics calculated from different temporal windows of the Landsat images across all habitat models (i.e. year-round, summer and winter models).

habitats (e.g. croplands or built-up areas) by lynx (Bouyer et al. 2015; Magg et al. 2015; Filla et al. 2017). Likewise, phenology metrics characterizing forage availability and quality were important predictors in our habitat models for red and roe deer. This is in line with previous studies demonstrating the effectiveness of satellite-derived phenology-information for characterizing ungulate habitat (Pettorelli et al. 2007; Merkle et al. 2016), and the finding that habitat selection by roe deer in our study area is largely driven by forage availability (Dupke et al. 2016). Moreover, metrics calculated from start-of-season observations showed the largest relative importance in our models. This corroborates findings on the effectiveness of characterizing spring conditions for capturing habitat features for large herbivores (Pettorelli et al. 2006, 2007; Hamel et al. 2009), particularly in temperate forests (Borowik et al. 2013).

Snow-cover metrics were important predictors in many of our habitat models. While the importance of snow-cover variables was particularly high in our winter models, they also showed considerably high importance scores in some of our summer models. This is likely since snow-cover distribution in winter is correlated with other factors influencing habitat quality in our study area. For example, areas with high snow cover tend to be located at higher elevations where higher levels of natural forest disturbance are found (Oeser et al. 2017), and disturbed forest stands are important habitat features for lynx, red deer and roe deer (Heurich et al. 2015; Filla et al. 2017). While numerous habitat studies have used snow-cover variables from coarse-resolution sensors such as MODIS (Hebblewhite et al. 2011; Kuemmerle et al. 2014; Michaud et al. 2014), our study highlights the underused potential of Landsat imagery in this context (Macander et al. 2015; Niittynen and Luoto 2018; Niittynen et al. 2018).

Despite these potential benefits of habitat metrics, some limitations need to be mentioned. First, while our habitat metrics allow characterizing different habitat aspects that manifest in spectral properties, there are several factors typically influencing habitat quality that our metrics cannot easily capture (e.g. human disturbance or competition with other species). Whereas including such additional predictors will improve models, we did not do so since

this would have hindered the direct comparison of the habitat metrics with land-cover maps for the purpose of habitat modeling. Second, interpreting the relationships between habitat metrics and habitat use can be difficult without reference information, since these relationships are often indirect (Bradley and Fleishman 2008). Other continuous satellite-based variables that are directly related to vegetation structure, such as fractional tree or shrub cover (Baumann et al. 2018), or biophysical variables, such as the leaf area index or the fraction of absorbed photosynthetically-active radiation (Viña et al. 2008), can provide more ecologically meaningful habitat information. However, the creation of such datasets is typically based on statistical models and thus, like land-cover mapping, requires reference information for training and validation. Fourth, we selected the temporal windows used for calculating metrics to capture phenological stages at our study site. Adapting the temporal windows to local phenology (Remelgado et al. 2018) or using metric definitions that allow comparing values across different phenological curves (e.g. highest/lowest quarterly median; Coops et al. 2008; Hijmans et al. 2005) might be necessary when transferring our approach to other regions. Finally, for areas and temporal windows with very high levels of cloud cover, some of our spectral-temporal metrics exhibited striping artifacts relating to scan line errors of Landsat 7. Integrating Landsat imagery with data from other sensors, such as Sentinel 2 (Wulder et al. 2015; Claverie et al. 2018) has the potential to reduce impacts of data gaps and further improve the ability to capture seasonal habitat dynamics.

Overall, our study highlights the considerable potential of spectral-temporal metrics from medium-resolution satellite imagery for monitoring, managing and conserving wildlife. A key advantage of Landsat in this regard lies in the global availability of 30 m-resolution imagery since the 1980s (at lower spatial resolutions even since the 1970s; Wulder et al. 2019). This offers great flexibility in terms of generating consistent predictors for habitat modeling across space and time and matching predictor data with available species records. This extraordinary potential for assessing habitat across large areas (Hansen and Loveland 2012) and long time periods (Kerr and Ostrovsky 2003; Vogelmann et al. 2012; Kennedy et al. 2014) has so far not been fully exploited (but see Jantz et al. 2016). The approach introduced in this study can help bridging this gap, opening up new possibilities to monitor spatiotemporal habitat dynamics based on Landsat imagery. Finally, further integrating the rich information of satellite image archives with habitat models has great potential to advance global biodiversity monitoring, as targeted by the Essential Biodiversity Variables framework (Pereira et al. 2013; Pettorelli et al. 2016; Jetz et al. 2019).

Acknowledgments

Julian Oeser gratefully acknowledges financial support from the Elsa-Neumann scholarship of the Federal State of Berlin. The GPS telemetry data was obtained by a study about predator-prey relationships of Eurasian lynx, red deer and roe deer carried out by the Bavarian Forest National Park Administration, Department of Research and Documentation, and a long-term research project on the Eurasian lynx in the Šumava National Park. Financial support was provided by EU Program Interreg IV (Objective 3: Czech Republic – the Independent State of Bavaria) and by IGA CZU 2011 4315013123113. We would like to thank L. Bufka, K. Mayer, O.Vojtěch, J. Mokrý, H. Burghart, M. Gahbauer and many other colleagues from the Šumava and Bavarian Forest National Parks for their help during the fieldwork. Moreover, we thank the editor and four reviewers for very valuable insights and guidance that improved this paper.

Data accessibility

A repository containing a Google Earth Engine script demonstrating the calculation of the Landsat-based habitat metrics used in this study is available under this link: https://code.earthengine.google.com/?accept_repo=users/julianoeser/Oeser_et_al_2019_Habitat_metrics.

References

Azzari, G., and D. B. Lobell. 2017. Landsat-based classification in the cloud: an opportunity for a paradigm shift in land cover monitoring. *Remote Sens. Environ.* **202**, 64–74.

Baumann, M., C. Levers, L. Macchi, H. Bluhm, B. Waske, N. I. Gasparri, et al. 2018. Mapping continuous fields of tree and shrub cover across the Gran Chaco using Landsat 8 and Sentinel-1 data. *Remote Sens. Environ.* **216**, 201–211.

Belotti, E., N. Weder, L. Bufka, A. Kaldhusdal, H. Küchenhoff, H. Seibold, et al. 2015. Patterns of lynx predation at the interface between protected areas and multi-use landscapes in Central Europe. *PLoS ONE* **10**, e0138139.

Bischof, R., L. E. Loe, E. L. Meisingset, B. Zimmermann, B. Van Moorter, and A. Mysterud. 2012. A migratory northern ungulate in the pursuit of spring: jumping or surfing the green wave? *Am. Nat.* **180**, 407–424.

Bleyhl, B., M. Baumann, P. Griffiths, A. Heidelberg, K. Manvelyan, V. C. Radeloff, et al. 2017. Assessing landscape connectivity for large mammals in the Caucasus using Landsat 8 seasonal image composites. *Remote Sens. Environ.* **193**, 193–203.

Borowik, T., N. Pettorelli, L. Sönnichsen, and B. Jędrzejewska. 2013. Normalized difference vegetation index (NDVI) as a predictor of forage availability for ungulates in forest and field habitats. *Eur. J. Wildl. Res.* **59**, 675–682.

Bouyer, Y., G. San Martin, P. Poncin, R. C. Beudels-Jamar, J. Odden, and J. D. C. Linnell. 2015. Eurasian lynx habitat selection in human-modified landscape in Norway: effects of different human habitat modifications and behavioral states. *Biol. Cons.* **191**, 291–299.

Boyce, M. S., and L. L. McDonald. 1999. Relating populations to habitats using resource selection functions. *Trends Ecol. Evol.* **14**, 268–272.

Bradley, B. A., and E. Fleishman. 2008. Can remote sensing of land cover improve species distribution modelling? *J. Biogeogr.* **35**, 1158–1159.

Brambilla, M., and F. Saporetti. 2014. Modelling distribution of habitats required for different uses by the same species: implications for conservation at the regional scale. *Biol. Cons.* **174**, 39–46.

Branton, M., and J. S. Richardson. 2011. Assessing the value of the umbrella-species concept for conservation planning with meta-analysis. *Conserv. Biol.* **25**, 9–20.

Breiman, L. 2001. Random forests. *Mach. Learn* **45**, 5–32.

Büttner, G., J. Feranec, G. Jaffrain, L. Mari, G. Maucha, and T. Soukup. 2004. The CORINE land cover 2000 project. *EARSeL eProceedings* **3**, 331–346.

Cardillo, M., G. M. Mace, K. E. Jones, J. Bielby, O. R. Bininda-Emonds, W. Sechrest, et al. 2005. Multiple causes of high extinction risk in large mammal species. *Science* **309**, 1239–1241.

Carroll, C., R. F. Noss, and P. C. Paquet. 2001. Carnivores as focal species for conservation planning in the Rocky Mountain region. *Ecol. Appl.* **11**, 961–980.

Claverie, M., J. Ju, J. G. Masek, J. L. Dungan, E. F. Vermote, J.-C. Roger, et al. 2018. The Harmonized Landsat and Sentinel-2 surface reflectance data set. *Remote Sens. Environ.* **219**, 145–161.

Clucas, B., K. McHugh, and T. Caro. 2008. Flagship species on covers of US conservation and nature magazines. *Biodivers. Conserv.* **17**, 1517.

Cohen, W. B., T. A. Spies, and M. Fiorella. 1995. Estimating the age and structure of forests in a multi-ownership landscape of western Oregon, U.S.A. *Int. J. Remote Sens.* **16**, 721–746.

Coops, N. C., and M. A. Wulder. 2019. Breaking the Habit (at). *Trends Ecol. Evol.* **34**, 585–587.

Coops, N. C., M. A. Wulder, D. C. Duro, T. Han, and S. Berry. 2008. The development of a Canadian dynamic habitat index using multi-temporal satellite estimates of canopy light absorbance. *Ecol. Ind.* **8**, 754–766.

Coops, N. C., M. A. Wulder, and D. Iwanicka. 2009. Demonstration of a satellite-based index to monitor habitat at continental-scales. *Ecol. Ind.* **9**, 948–958.

Cord, A., and D. Rödder. 2011. Inclusion of habitat availability in species distribution models through multi-temporal remote-sensing data? *Ecol. Appl.* **21**, 3285–3298.

Cord, A. F., D. Klein, F. Mora, and S. Dech. 2014. Comparing the suitability of classified land cover data and remote sensing variables for modeling distribution patterns of plants. *Ecol. Model.* **272**, 129–140.

Crist, E. P. 1985. A TM Tasseled Cap equivalent transformation for reflectance factor data'. *Remote Sens. Environ.* **17**, 301–306.

Crist, E. P., and R. C. Cicone. 1984. A physically-based transformation of Thematic Mapper data - the TM Tasseled Cap. *IEEE Trans. Geosci. Remote Sens.* **GE-22**, 256–263.

De Jong, S. M. 1994. Derivation of vegetative variables from a Landsat TM image for modelling soil erosion. *Earth Surf. Proc. Land.* **19**, 165–178.

Dupke, C., C. Bonenfant, B. Reineking, R. Hable, T. Zeppenfeld, M. Ewald, et al. 2016. Habitat selection by a large herbivore at multiple spatial and temporal scales is primarily governed by food resources. *Ecography* **40**, 1014–1027.

Dwyer, J., D. Roy, B. Sauer, C. Jenkerson, H. Zhang, and L. Lymburner. 2018. Analysis ready data: enabling analysis of the landsat archive. *Remote Sens.* **10**, 1363.

Elith, J., and J. R. Leathwick. 2009. Species distribution models: ecological explanation and prediction across space and time. *Annu. Rev. Ecol. Evol. Syst.* **40**, 677–697.

Elith, J., C. H. Graham, R. P. Anderson, M. Dudík, S. Ferrier, A. Guisan, et al. 2006. Novel methods improve prediction of species' distributions from occurrence data. *Ecography* **29**, 129–151.

Fernandes, R., and G. S. Leblanc. 2005. Parametric (modified least squares) and non-parametric (Theil–Sen) linear regressions for predicting biophysical parameters in the presence of measurement errors. *Remote Sens. Environ.* **95**, 303–316.

Filla, M., J. Premier, N. Magg, C. Dupke, I. Khorozyan, M. Waltert, et al. 2017. Habitat selection by Eurasian lynx (Lynx lynx) is primarily driven by avoidance of human activity during day and prey availability during night. *Ecol. Evol.* **7**, 6367–6381.

Flood, N. 2013. Seasonal Composite Landsat TM/ETM+ Images Using the Medoid (a Multi-Dimensional Median). *Remote Sens.* **5**, 6481–6500.

Foga, S., P. L. Scaramuzza, S. Guo, Z. Zhu, R. D. Dilley, T. Beckmann, et al. 2017. Cloud detection algorithm comparison and validation for operational Landsat data products. *Remote Sens. Environ.* **194**, 379–390.

Frans, V. F., A. A. Augé, H. Edelhoff, S. Erasmi, N. Balkenhol, and J. O. Engler. 2017. Quantifying apart what belongs together: a multi-state species distribution modelling framework for species using distinct habitats. *Methods Ecol. Evol.* **9**, 98–108.

Godvik, I. M. R., L. E. Loe, J. O. Vik, V. Veiberg, R. Langvatn, and A. Mysterud. 2009. Temporal scales, trade-offs, and functional responses in red deer habitat selection. *Ecology* **90**, 699–710.

Gómez, C., J. C. White, and M. A. Wulder. 2016. Optical remotely sensed time series data for land cover classification: a review. *ISPRS J. Photogramm. Remote Sens.* **116**, 55–72.

Gonzalez, S. R., H. Latifi, H. Weinacker, M. Dees, B. Koch, and M. Heurich. 2018. Integrating LiDAR and high-resolution imagery for object-based mapping of forest habitats in a heterogeneous temperate forest landscape. *Int. J. Remote Sens.* **39**, 1–26.

Gorelick, N., M. Hancher, M. Dixon, S. Ilyushchenko, D. Thau, and R. Moore. 2017. Google Earth Engine: planetary-scale geospatial analysis for everyone. *Remote Sens. Environ.* **202**, 18–27.

Götmark, F., Å. Berglund, and K. Wiklander. 2005. Browsing damage on broadleaved trees in semi-natural temperate forest in Sweden, with a focus on oak regeneration. *Scand. J. For. Res.* **20**, 223–234.

Griffiths, P., S. v. d. Linden, T. Kuemmerle, and P. Hostert. 2013. A pixel-based Landsat compositing algorithm for large area land cover mapping. *IEEE J. Select. Topics Appl. Earth Obs. Remote Sens.* **6**, 2088–2101.

Gschweng, M., K. V. Kalko Elisabeth, P. Berthold, W. Fiedler, and J. Fahr. 2012. Multi-temporal distribution modelling with satellite tracking data: predicting responses of a long-distance migrant to changing environmental conditions. *J. Appl. Ecol.* **49**, 803–813.

Guisan, A., and W. Thuiller. 2005. Predicting species distribution: offering more than simple habitat models. *Ecol. Lett.* **8**, 993–1009.

Guisan, A., and N. E. Zimmermann. 2000. Predictive habitat distribution models in ecology. *Ecol. Model.* **135**, 147–186.

Hall, D. K., G. A. Riggs, J. L. Foster, and S. V. Kumar. 2010. Development and evaluation of a cloud-gap-filled MODIS daily snow-cover product. *Remote Sens. Environ.* **114**, 496–503.

Hamel, S., M. Garel, M. Festa-Bianchet, J.-M. Gaillard, and S. D. Côté. 2009. Spring Normalized Difference Vegetation Index (NDVI) predicts annual variation in timing of peak faecal crude protein in mountain ungulates. *J. Appl. Ecol.* **46**, 582–589.

Hansen, M. C., and T. R. Loveland. 2012. A review of large area monitoring of land cover change using Landsat data. *Remote Sens. Environ.* **122**, 66–74.

Hansen, M. J., S. E. Franklin, C. Woudsma, and M. Peterson. 2001. Forest structure classification in the North Columbia Mountains using the Landsat TM Tasseled Cap wetness component. *Can. J. Remote. Sens.* **27**, 20–32.

Hansen, M. C., A. Egorov, P. V. Potapov, S. V. Stehman, A. Tyukavina, S. A. Turubanova, et al. 2014. Monitoring conterminous United States (CONUS) land cover change with Web-Enabled Landsat Data (WELD). *Remote Sens. Environ.* **140**, 466–484.

He, K. S., B. A. Bradley, A. F. Cord, D. Rocchini, M.-N. Tuanmu, S. Schmidtlein, et al. 2015. Will remote sensing shape the next generation of species distribution models? *Remote Sens Ecol Conserv* **1**, 4–18.

Hebblewhite, M., D. G. Miquelle, A. A. Murzin, V. V. Aramilev, and D. G. Pikunov. 2011. Predicting potential habitat and population size for reintroduction of the Far Eastern leopards in the Russian Far East. *Biol. Cons.* **144**, 2403–2413.

Heinze, E., S. Boch, M. Fischer, D. Hessenmöller, B. Klenk, J. Müller, et al. 2011. Habitat use of large ungulates in northeastern Germany in relation to forest management. *For. Ecol. Manage.* **261**, 288–296.

Heurich, M., T. T. G. Brand, M. Y. Kaandorp, P. Šustr, J. Müller, and B. Reineking. 2015. Country, cover or protection: what shapes the distribution of red deer and roe deer in the Bohemian Forest Ecosystem? *PLoS ONE* **10**, e0120960.

Hijmans, R. J., S. E. Cameron, J. L. Parra, P. G. Jones, and A. Jarvis. 2005. Very high resolution interpolated climate surfaces for global land areas. *Int. J. Climatol.* **25**, 1965–1978.

Hijmans, R. J., S. Phillips, J. Leathwick, and J. Elith. 2017. *dismo: Species distribution modeling. R package version 1.1-4*. The R Foundation for Statistical Computing, Vienna.

Hirzel, A. H., G. Le Lay, V. Helfer, C. Randin, and A. Guisan. 2006. Evaluating the ability of habitat suitability models to predict species presences. *Ecol. Model.* **199**, 142–152.

Holbrook, J. D., J. R. Squires, L. E. Olson, R. L. Lawrence, and S. L. Savage. 2017. Multiscale habitat relationships of snowshoe hares (Lepus americanus) in the mixed conifer landscape of the Northern Rockies, USA: cross-scale effects of horizontal cover with implications for forest management. *Ecol. Evol.* **7**, 125–144.

Holloway, P., and J. A. Miller. 2017. A quantitative synthesis of the movement concepts used within species distribution modelling. *Ecol. Model.* **356**, 91–103.

Jantz, M. S., L. Pintea, J. Nackoney, and C. M. Hansen. 2016. Landsat ETM+ and SRTM data provide near real-time monitoring of chimpanzee (Pan troglodytes) habitats in Africa. *Remote Sens.* **8**, 427.

Jetz, W., M. A. McGeoch, R. Guralnick, S. Ferrier, J. Beck, M. J. Costello, et al. 2019. Essential biodiversity variables for mapping and monitoring species populations. *Nat Ecol Evol* **3**, 539–551.

Jiménez-Valverde, A., P. Acevedo, A. M. Barbosa, J. M. Lobo, and R. Real. 2013. Discrimination capacity in species distribution models depends on the representativeness of the environmental domain. *Glob. Ecol. Biogeogr.* **22**, 508–516.

Jin, S., and S. A. Sader. 2005. Comparison of time series tasseled cap wetness and the normalized difference moisture index in detecting forest disturbances. *Remote Sens. Environ.* **94**, 364–372.

Kays, R., M. C. Crofoot, W. Jetz, and M. Wikelski. 2015. Terrestrial animal tracking as an eye on life and planet. *Science* **348**, aaa2478.

Kennedy, R. E., S. Andréfouët, W. B. Cohen, C. Gómez, P. Griffiths, M. Hais, et al. 2014. Bringing an ecological view of change to Landsat-based remote sensing. *Front. Ecol. Environ.* **12**, 339–346.

Kerr, J. T., and M. Ostrovsky. 2003. From space to species: ecological applications for remote sensing. *Trends Ecol. Evol.* **18**, 299–305.

Krishnaswamy, J., K. S. Bawa, K. N. Ganeshaiah, and M. C. Kiran. 2009. Quantifying and mapping biodiversity and ecosystem services: utility of a multi-season NDVI based Mahalanobis distance surrogate. *Remote Sens. Environ.* **113**, 857–867.

Krojerová-Prokešová, J., M. Barančeková, P. Šustr, and M. Heurich. 2010. Feeding patterns of red deer Cervus elaphus along an altitudinal gradient in the Bohemian Forest: effect of habitat and season. *Wildl Biol* **16**, 173–184.

Kuemmerle, T., K. Perzanowski, O. Chaskovskyy, K. Ostapowicz, L. Halada, A.-T. Bashta, et al. 2010. European Bison habitat in the Carpathian Mountains. *Biol. Cons.* **143**, 908–916.

Kuemmerle, T., L. Baskin, P. J. Leitão, A. V. Prishchepov, K. Thonicke, and V. C. Radeloff. 2014. Potential impacts of oil and gas development and climate change on migratory reindeer calving grounds across the Russian Arctic. *Diversity Distrib.* **20**, 416–429.

Kuemmerle, T., C. Levers, B. Bleyhl, W. Olech, K. Perzanowski, C. Reusch, et al. 2018. One size does not fit all: European bison habitat selection across herds and spatial scales. *Landscape Ecol.* **33**, 1559–1572.

Kullberg, Y., and R. Bergström. 2001. Winter browsing by large herbivores on planted deciduous seedlings in Southern Sweden. *Scand. J. For. Res.* **16**, 371–378.

Lahoz-Monfort, J. J., G. Guillera-Arroita, E. J. Milner-Gulland, R. P. Young, and E. Nicholson. 2010. Satellite imagery as a single source of predictor variables for habitat suitability modelling: how Landsat can inform the conservation of a critically endangered lemur. *J. Appl. Ecol.* **47**, 1094–1102.

Larson, M. A., F. R. Thompson, J. J. Millspaugh, W. D. Dijak, and S. R. Shifley. 2004. Linking population viability, habitat suitability, and landscape simulation models for conservation planning. *Ecol. Model.* **180**, 103–118.

Leitão, P. J., and M. J. Santos. 2019. Improving models of species ecological niches: a remote sensing overview. *Front Ecol Evol* **7**, 9.

Macander, M. J., C. S. Swingley, K. Joly, and M. K. Raynolds. 2015. Landsat-based snow persistence map for northwest Alaska. *Remote Sens. Environ.* **163**, 23–31.

Magg, N., J. Müller, C. Heibl, K. Hackländer, S. Wölfl, M. Wölfl, et al. 2015. Habitat availability is not limiting the distribution of the Bohemian-Bavarian lynx Lynx lynx population. *Oryx* **50**, 742–752.

Margules, C. R., and R. L. Pressey. 2000. Systematic conservation planning. *Nature* **405**, 243–253.

Masek, J. G., E. F. Vermote, N. E. Saleous, R. Wolfe, F. G. Hall, K. F. Huemmrich, et al. 2006. A Landsat surface reflectance dataset for North America, 1990-2000. *IEEE Geosci. Remote Sens. Lett.* **3**, 68–72.

McDermid, G. J., S. E. Franklin, and E. F. LeDrew. 2005. Remote sensing for large-area habitat mapping. *Prog. Phys. Geogr.* **29**, 449–474.

Merkle, J. A., K. L. Monteith, E. O. Aikens, M. M. Hayes, K. R. Hersey, A. D. Middleton, et al. 2016. Large herbivores surf waves of green-up during spring. *Proc Biol Sci* **283**: 20160456.

Merow, C., M. J. Smith, and J. A. Silander. 2013. A practical guide to MaxEnt for modeling species' distributions: what it does, and why inputs and settings matter. *Ecography* **36**, 1058–1069.

Michaud, J.-S., N. C. Coops, M. E. Andrew, M. A. Wulder, G. S. Brown, and G. J. M. Rickbeil. 2014. Estimating moose (Alces alces) occurrence and abundance from remotely derived environmental indicators. *Remote Sens. Environ.* **152**, 190–201.

Nagendra, H., R. Lucas, J. P. Honrado, R. H. G. Jongman, C. Tarantino, M. Adamo, et al. 2013. Remote sensing for conservation monitoring: assessing protected areas, habitat extent, habitat condition, species diversity, and threats. *Ecol. Ind.* **33**, 45–59.

Niittynen, P., and M. Luoto. 2018. The importance of snow in species distribution models of arctic vegetation. *Ecography* **41**, 1024–1037.

Niittynen, P., R. K. Heikkinen, and M. Luoto. 2018. Snow cover is a neglected driver of Arctic biodiversity loss. *Nat. Clim. Change*. https://doi.org/10.1038/s41558-018-0311-x

Northrup, J. M., M. B. Hooten, C. R. Jr Anderson, and G. Wittemyer. 2013. Practical guidance on characterizing availability in resource selection functions under a use–availability design. *Ecology* **94**, 1456–1463.

Oeser, J., D. Pflugmacher, C. Senf, M. Heurich, and P. Hostert. 2017. Using intra-annual landsat time series for attributing forest disturbance agents in Central Europe. *Forests* **8**, 251.

Pasquarella, V. J., C. E. Holden, L. Kaufman, and C. E. Woodcock. 2016. From imagery to ecology: leveraging time series of all available Landsat observations to map and monitor ecosystem state and dynamics. *Remote Sens Ecol Conserv* **2**, 152–170.

Pearson, R. G., T. P. Dawson, and C. Liu. 2004. Modelling species distributions in Britain: a hierarchical integration of climate and land-cover data. *Ecography* **27**, 285–298.

Pereira, H. M., S. Ferrier, M. Walters, G. N. Geller, R. H. G. Jongman, R. J. Scholes, et al. 2013. Essential biodiversity variables. *Science* **339**, 277–278.

Pettorelli, N., J. O. Vik, A. Mysterud, J.-M. Gaillard, C. J. Tucker, and N. C. Stenseth. 2005. Using the satellite-derived NDVI to assess ecological responses to environmental change. *Trends Ecol. Evol.* **20**, 503–510.

Pettorelli, N., J.-M. Gaillard, A. Mysterud, P. Duncan, N. Chr, D. Stenseth, et al. 2006. Using a proxy of plant productivity (NDVI) to find key periods for animal performance: the case of roe deer. *Oikos* **112**, 565–572.

Pettorelli, N., F. Pelletier, A. v. Hardenberg, M. Festa-Bianchet, and S. D. Côté. 2007. Early onset of vegetation growth vs. rapid green-up: impacts on juvenile mountain ungulates. *Ecology* **88**:381–390.

Pettorelli, N., S. Ryan, T. Mueller, N. Bunnefeld, B. Jędrzejewska, M. Lima, et al. 2011. The Normalized Difference Vegetation Index (NDVI) - unforeseen successes in animal ecology. *Clim. Res.* **46**, 15–27.

Pettorelli, N., M. Wegmann, A. Skidmore, S. Mücher, T. P. Dawson, M. Fernandez, et al. 2016. Framing the concept of satellite remote sensing essential biodiversity variables: challenges and future directions. *Remote Sens Ecol Conserv* **2**, 122–131.

Pflugmacher, D., O. N. Krankina, W. B. Cohen, M. A. Friedl, D. Sulla-Menashe, R. E. Kennedy, et al. 2011. Comparison and assessment of coarse resolution land cover maps for Northern Eurasia. *Remote Sens. Environ.* **115**, 3539–3553.

Pflugmacher, D., A. Rabe, M. Peters, and P. Hostert. 2019. Mapping pan-European land cover using Landsat spectral-temporal metrics and the European LUCAS survey. *Remote Sens. Environ.* **221**, 583–595.

Phillips, S. J., and M. Dudík. 2008. Modeling of species distributions with Maxent: new extensions and a comprehensive evaluation. *Ecography* **31**, 161–175.

Phillips, S. J., and J. Elith. 2010. POC plots: calibrating species distribution models with presence-only data. *Ecology* **91**, 2476–2484.

Phillips, S. J., R. P. Anderson, and R. E. Schapire. 2006. Maximum entropy modeling of species geographic distributions. *Ecol. Model.* **190**, 231–259.

Pimm, S. L., S. Alibhai, R. Bergl, A. Dehgan, C. Giri, Z. Jewell, et al. 2015. Emerging technologies to conserve biodiversity. *Trends Ecol. Evol.* **30**, 685–696.

Potapov, P., S. Turubanova, and M. C. Hansen. 2011. Regional-scale boreal forest cover and change mapping using Landsat data composites for European Russia. *Remote Sens. Environ.* **115**, 548–561.

Powell, R. L., N. Matzke, C. de Souza, M. Clark, I. Numata, L. L. Hess, et al. 2004. Sources of error in accuracy assessment of thematic land-cover maps in the Brazilian Amazon. *Remote Sens. Environ.* **90**, 221–234.

Pressey, R. L., M. Cabeza, M. E. Watts, R. M. Cowling, and K. A. Wilson. 2007. Conservation planning in a changing world. *Trends Ecol. Evol.* **22**, 583–592.

Remelgado, R., B. Leutner, K. Safi, R. Sonnenschein, C. Kuebert, and M. Wegmann. 2018. Linking animal movement and remote sensing – mapping resource suitability from a remote sensing perspective. *Remote Sens Ecol Conserv* **4**, 211–224.

Ripple, W. J., J. A. Estes, R. L. Beschta, C. C. Wilmers, E. G. Ritchie, M. Hebblewhite, et al. 2014. Status and ecological effects of the world's largest carnivores. *Science* **343**, 6167.

Ripple, W. J., T. M. Newsome, C. Wolf, R. Dirzo, K. T. Everatt, M. Galetti, et al. 2015. Collapse of the world's largest herbivores. *Sci Adv* **1**, e1400103.

Rivrud, M. I., M. Heurich, P. Krupczynski, J. Müller, and A. Mysterud. 2016. Green wave tracking by large herbivores: an experimental approach. *Ecology* **97**, 3547–3553.

Roy, P. S., and S. A. Ravan. 1996. Biomass estimation using satellite remote sensing data—An investigation on possible approaches for natural forest. *J. Biosci.* **21**, 535–561.

Roy, D. P., V. Kovalskyy, H. K. Zhang, E. F. Vermote, L. Yan, S. S. Kumar, et al. 2016. Characterization of Landsat-7 to Landsat-8 reflective wavelength and normalized difference vegetation index continuity. *Remote Sens. Environ.* **185**, 57–70.

Schadt, S., E. Revilla, T. Wiegand, F. Knauer, P. Kaczensky, U. Breitenmoser, et al. 2002. Assessing the suitability of central European landscapes for the reintroduction of Eurasian lynx. *J. Appl. Ecol.* **39**, 189–203.

Searcy, C. A., and H. B. Shaffer. 2016. Do ecological niche models accurately identify climatic determinants of species ranges? *Am. Nat.* **187**, 423–435.

Senf, C., D. Pflugmacher, M. Heurich, and T. Krueger. 2017. A Bayesian hierarchical model for estimating spatial and temporal variation in vegetation phenology from Landsat time series. *Remote Sens. Environ.* **194**, 155–160.

Sergio, F., I. A. N. Newton, L. Marchesi, and P. Pedrini. 2006. Ecologically justified charisma: preservation of top predators delivers biodiversity conservation. *J. Appl. Ecol.* **43**, 1049–1055.

Shirley, S. M., Z. Yang, R. A. Hutchinson, J. D. Alexander, K. McGarigal, and M. G. Betts. 2013. Species distribution modelling for the people: unclassified Landsat TM imagery predicts bird occurrence at fine resolutions. *Divers. Distrib.* **19**, 855–866.

Sutherland, W. J., A. S. Pullin, P. M. Dolman, and T. M. Knight. 2004. The need for evidence-based conservation. *Trends Ecol. Evol.* **19**, 305–308.

Theil, H. 1992. A rank-invariant method of linear and polynomial regression analysis. Pp. 345–381 in B. Raj and J. Koerts, eds. *Henri theil's contributions to economics and econometrics: econometric theory and methodology*. Springer, Netherlands, Dordrecht.

Thuiller, W., M. B. Araújo, and S. Lavorel. 2004. Do we need land-cover data to model species distributions in Europe? *J. Biogeogr.* **31**, 353–361.

Treves, A., and K. U. Karanth. 2003. Human-carnivore conflict and perspectives on carnivore management worldwide. *Conserv. Biol.* **17**, 1491–1499.

Vermote, E., C. Justice, M. Claverie, and B. Franch. 2016. Preliminary analysis of the performance of the Landsat 8/OLI land surface reflectance product. *Remote Sens. Environ.* **185**, 46–56.

Viña, A., S. Bearer, H. Zhang, Z. Ouyang, and J. Liu. 2008. Evaluating MODIS data for mapping wildlife habitat distribution. *Remote Sens. Environ.* **112**, 2160–2169.

Vogelmann, J. E., G. Xian, C. Homer, and B. Tolk. 2012. Monitoring gradual ecosystem change using Landsat time series analyses: case studies in selected forest and rangeland ecosystems. *Remote Sens. Environ.* **122**, 92–105.

West, A. M., P. H. Evangelista, C. S. Jarnevich, S. Kumar, A. Swallow, M. W. Luizza, et al. 2017. Using multi-date satellite imagery to monitor invasive grass species distribution in post-wildfire landscapes: an iterative, adaptable approach that employs open-source data and software. *Int. J. Appl. Earth Obs. Geoinf.* **59**, 135–146.

Wölfl, M., L. Bufka, J. Červený, P. Koubek, M. Heurich, H. Habel, et al. 2001. Distribution and status of lynx in the border region between Czech Republic, Germany and Austria. *Acta Theriologica* **46**, 181–194.

Wulder, M. A., T. Hilker, J. C. White, N. C. Coops, J. G. Masek, D. Pflugmacher, et al. 2015. Virtual constellations for global terrestrial monitoring. *Remote Sens. Environ.* **170**, 62–76.

Wulder, M. A., J. C. White, T. R. Loveland, C. E. Woodcock, A. S. Belward, W. B. Cohen, et al. 2016. The global Landsat archive: Status, consolidation, and direction. *Remote Sens. Environ.* **185**, 271–283.

Wulder, M. A., N. C. Coops, D. P. Roy, J. C. White, and T. Hermosilla. 2018. Land cover 2.0. *Int. J. Remote Sens.* **39**, 4254–4284.

Wulder, M. A., T. R. Loveland, D. P. Roy, C. J. Crawford, J. G. Masek, C. E. Woodcock, et al. 2019. Current status of Landsat program, science, and applications. *Remote Sens. Environ.* **225**, 127–147.

Yang, X., and Z. Liu. 2005. Use of satellite-derived landscape imperviousness index to characterize urban spatial growth. *Comput. Environ. Urban Syst.* **29**, 524–540.

Young, J., A. Watt, P. Nowicki, D. Alard, J. Clitherow, K. Henle, et al. 2005. Towards sustainable land use: identifying and managing the conflicts between human activities and biodiversity conservation in Europe. *Biodivers. Conserv.* **14**, 1641–1661.

Young, N. E., R. S. Anderson, S. M. Chignell, A. G. Vorster, R. Lawrence, and P. H. Evangelista. 2017. A survival guide to Landsat preprocessing. *Ecology* **98**, 920–932.

Zeller, K. A., K. McGarigal, and A. R. Whiteley. 2012. Estimating landscape resistance to movement: a review. *Landscape Ecol.* **27**, 777–797.

Zuckerberg, B., D. Fink, F. A. La Sorte, W. M. Hochachka, and S. Kelling. 2016. Novel seasonal land cover associations for eastern North American forest birds identified through dynamic species distribution modelling. *Divers. Distrib.* **22**, 717–730.

Supporting Information

Additional supporting information may be found online in the Supporting Information section at the end of the article.

Figure S1. Strength of correlation between Landsat habitat metrics of different metric groups, expressed as absolute Pearson correlation coefficients. Within-group correlation refers to correlation coefficients of all metrics belonging to a given group, out-of-group correlation refers to correlation coefficients of metrics of a given group with metrics not belonging to that group.

Figure S2. Comparison of Landsat-based snow-cover frequency metrics with average snow cover derived from MODIS daily snow cover. While both datasets show similar spatial patterns, values of the Landsat metrics were higher in areas with high snow cover. Moreover, striping artefacts relating to Landsat 7 scan line errors are visible in the Landsat-based metrics.

Figure S3. Scatterplots between the Landsat snow-cover frequency metrics and average snow-cover values from MODIS 10A1 snow-cover product, based on observations from (A) the entire year, and (B) only start of season observations. Landsat metrics were resampled to 500 m resolution of the MODIS data to allow comparison. Blue line indicates slope of linear regression between both datasets, black line indicates perfect agreement between values.

Figure S4. Land-cover map produced for the area around the study region. Black lines show national park borders; black dashed lines indicate country borders. Grey dashed line show the extent of the study region for which habitat suitability maps were created.

Figure S5. Habitat suitability maps of summer habitat models using the habitat metrics (left column), the site-specific land-cover map (middle column) and the CORINE land-cover map (right column) for lynx, red deer and roe deer. Continuous line indicates country border, dashed lines show the extents of the national parks.

Figure S6. Habitat suitability maps based on winter habitat models using the habitat metrics (left column), our own land-cover map (middle column) and the CORINE land-cover map (right column) for lynx, red deer and roe deer. Continuous line indicates country border, dashed lines show the extents of the national parks.

Figure S7. Productivity metrics (median of Tasseled Cap greenness) calculated based on start-of-season, peak-of-season and end-of-season observations (see Landsat-based habitat metrics in main text). Striping artefacts mainly occurred in metrics calculated from start-of-season observations, which was the temporal window with the fewest number of available images, and the strongest influence of cloud cover.

Figure S8. Variation of metric values (by metric groups) with vegetation classes relating to forest structure: (A) Deadwood and (B) Forest regrowth. All metrics were standardized via a z-Transformation to allow comparability between different spectral indices.

Table S1. Map accuracies and area estimates for our Landsat-based land-cover map. All numbers are sampling-bias-adjusted and are given with 95% confidence intervals.

Table S2. Overview of CORINE classes present in our study area. Columns refer to different levels of thematic detail used in the CORINE class nomenclature. Classes were used at highest thematic detail (i.e. LEVEL 1) in our habitat models.

